Inorg. Chem. **2002**, *41*, 913–922

DNA Hydrolytic Cleavage by the Diiron(III) Complex $Fe_2(DTPB)(\mu\text{-}O)(\mu\text{-}Ac)Cl(BF_4)_2$: Comparison with Other Binuclear Transition Metal Complexes

Changlin Liu,*,† Siwang Yu,† Dongfeng Li,‡ Zhanru Liao,‡ Xiaohui Sun,† and Huibi Xu†

Department of Chemistry, Huazhong University of Science and Technology, Wuhan 430074, China, and Department of Chemistry, Central China Normal University, Wuhan 430070, China

Received March 19, 2001

The binuclear structure of $Fe_2(DTPB)(\mu\text{-}O)(\mu\text{-}Ac)Cl(BF_4)_2$ (DTPB = 1,1,4,7,7-penta (2′-benzimidazol-2-ylmethyl)-triazaheptane, Ac = acetate) was characterized by UV–visible absorption and infrared spectra and NMR and ESR. The binding interaction of DNA with the diiron complex was examined spectroscopically. Supercoiled and linear DNA hydrolytic cleavage by the diiron complex is supported by the evidence from anaerobic reactions, free radical quenching, high performance liquid chromatography experiments, and enzymatic manipulation such as T4 ligase ligation, 5′-^{32}P end-labeling, and footprinting analysis. The estimation of rate for the supercooiled DNA double strand cleavage shows one of the largest known rate enhancement factors, $\sim 10^{10}$ against DNA. Moreover, the DNA hydrolysis chemistry needs no coreactant such as hydrogen peroxide. The poor sequence-specific DNA cleavage indicated by the restriction analysis of the pBR322 DNA linearized by the diiron complex might be due to the diiron complex bound to DNA by a coordination of its two ferric ions to the DNA phosphate oxygens, as suggested by spectral characterizations. The hydrolysis chemistry for a variety of binuclear metal complexes including $Fe_2(DTPB)(\mu\text{-}O)(\mu\text{-}Ac)Cl(BF_4)_2$ is compared. It is established that the dominant factors for the DNA hydrolysis activities of the binuclear metal complexes are the μ-oxo bridge, labile and anionic ligands, and open coordination site(s). Concerning the hydrolytic mechanisms, the diiron complex $Fe_2(DTPB)(\mu\text{-}O)(\mu\text{-}Ac)Cl(BF_4)_2$ might share many points in common with the native purple acid phosphatases.

Introduction

The development of reagents that can specifically recognize and cleave DNA and RNA under physiological conditions via oxidative and hydrolytic mechanisms has been attracting a great interest in the bioinorganic chemistry field.[1−5] Although many metal complexes have been successfully applied to RNA hydrolytic cleavage because of its highly efficient internal nucleophile (2′-OH),[2−11] there have been few reagents that can relatively cleave a double-stranded DNA with high hydrolytic stability.[12−20] This is a result of the repulsion between the negatively charged DNA phos-

* Author to whom correspondence should be addressed. E-mail: L20919@public.wh.hb.cn. Fax: 86-27-87543632.
† Huazhong University of Science and Technology.
‡ Central China Normal University.

(1) *Chem. Rev.* **1998**, *98*, 937−1262. Thematic issue on RNA/DNA cleavage, Bashkin, J. K., guest editor.
(2) William, N. H.; Takasaki, B.; Wall, M.; Chin, J. *Acc. Chem. Res.* **1999**, *32*, 485.
(3) Trawick, B. N.; Daniher, A. T.; Bashkin, J. K. *Chem. Rev.* **1998**, *98*, 939.
(4) Oivanan, M.; Kuusela, S.; Lönnberg, H. *Chem. Rev.* **1998**, *98*, 961.
(5) Hegg, E, L.; Deal, K. A.; Kiessling, L. L.; Burstyn, J. N. *Inorg. Chem.* **1997**, *36*, 1715.
(6) Yong, M. J.; Chin, J. *J. Am. Chem. Soc.* **1995**, *117*, 10577.
(7) Linkletter, B.; Chin, J. *Angew. Chem., Int. Ed. Engl.* **1995**, *34*, 472.
(8) Amin, S.; Morrow, J. R.; Lake, C. H.; Churchill, M. R. *Angew. Chem., Int. Ed. Engl.* **1994**, *33*, 773.
(9) Modak, A. S.; Gard, J. K.; Merriman, M. C.; Winkeler, K. A.; Bashkin, J. K.; Stern, M. K. *J. Am. Chem. Soc.* **1991**, *113*, 283.
(10) Magda, D.; Miller, R. A.; Sessler, J. L.; Iverson, B. L. *J. Am. Chem. Soc.* **1994**, *116*, 7439.
(11) Baker, B. F.; Khalili, H.; Wei, N.; Morrow, J. R. *J. Am. Chem. Soc.* **1997**, *119*, 8749.
(12) Rammo, J.; Hettich, R.; Roigk, A.; Schneider, H.-J. *Chem. Commun.* **1996**, 105.
(13) Dixon, N. E.; Geue, R. J.; Lambert, A. L.; Moghaddas, S.; Pearce, D. A.; Sargeson, A. M. *Chem. Commun.* **1996**, 1287.
(14) Basile, L. A.; Raphael, A. L.; Barton, J. K. *J. Am. Chem. Soc.* **1987**, *109*, 7550.
(15) Basile, L. A.; Barton, J. K. *J. Am. Chem. Soc.* **1987**, *109*, 7548.
(16) Fitzsimons, M. P.; Barton, J. K. *J. Am. Chem. Soc.* **1997**, *119*, 3379.
(17) Hettich, R.; Schneider, H.-J. *J. Am. Chem. Soc.* **1997**, *119*, 5638.
(18) Yashiro, M.; Ishikuno, A.; Komiyama, M. *Chem. Commun.* **1995,** 1793.

10.1021/ic010302h CCC: $22.00
Published on Web 01/23/2002

phatediester backbone and potential nucleophiles and the lack of 2′-OH as an internal nucleophile.[2,20] Consequently, DNA cleavage has been mainly focused on oxidative chemistry mediated by transition metal complexes.[1] Moreover, many oxidative cleavers and photocleavers have been utilized with great success for DNA footprinting,[21] positioning base mismatches, bulges and hairpin loops,[22] and determining conformational variation of DNA[23] and as chemotherapeutic agents.[1,24] However, because the radical-based oxidative cleavers require addition of external agents such as hydrogen peroxide and light to induce the cleavage reactions, and the products are not available for further enzymatic manipulation because of the lack of 3′-OH and 5′-OPO_3 ends,[1,25] their applications are remarkably limited in the fields of molecular biology and biotechnology. DNA hydrolytic cleavage does not suffer from these disadvantages. The DNA fragments generated by the hydrolytic cleavers can be enzymatically ligated and end-labeled. The metal complexes that catalyze DNA hydrolytic cleavage could be useful not only in gene manipulation but also in mimicking and elucidating the important roles of metal ions in metalloenzyme catalysis.

Metal ions and their mononuclear complexes hydrolyze DNA by activating phosphodiester bonds. The labile lanthanide ions[2,16,26−32] such as La^{3+}, Eu^{3+}, and Yb^{3+}, and, in particular, Ce^{4+}, can catalyze phosphodiester, nucleotide dimer, oligonucleotide, and supercoiled DNA hydrolysis. The nucleophilic and intercalative ligands such as polyamine, cryptand, and nitrogen-containing macrocycles can enhance the DNA cleavage activity catalyzed by La^{3+}, Eu^{3+}, and Yb^{3+}.[12,33] It is notable that there are a few examples of successful DNA hydrolytic cleavage by mononuclear metal complexes. Although ammonium-functionalized Cu^{2+} complexes are rapid phosphatediester hydrolytic cleavers, the substitutionally labile amine−Cu^{2+} or Zn^{2+} complexes and Zn^{2+} complexes of histidine-containing peptide are slower hydrolytic agents than the lanthanide complexes.[34−41] $[Ru(DIP)_2macro]^{n+}$[15] and $Rh(phi)_2bpy'$-peptide (DIP and phi = intercalative ligands; macro = chelator),[14] where complexes $Ru(DIP)_2$ and $Rh(phi)_2$ are specific metallointercalators in the DNA major groove, cleave hydrolytically DNA in the presence of certain divalent metal ions. Zinc ion allows the Rh intercalator−peptide complex to reach an optimum hydrolase activity.[16] The Co^{III} complexes of polyamine derivatives such as cyclen, trpn, and tamen can act as catalysts for the hydrolysis of phosphate esters and of DNA with a measurable 10 million-fold rate increase.[13,17] It was recently reported that the Cu^{II} complexes with macrocycles,[42] *cis*,*cis*-1, 3, 5-triaminocyclohexane[43] and neamine,[44] can efficiently promote the plasmid and phage DNA hydrolytic cleavage.

Currently, there are more and more frequent examples of catalytic systems based on two metal ions reported in chemistry[2] and in biochemistry, because many enzymes that catalyze phosphate ester hydrolysis are activated by two or more metal ions.[45,46] There is considerable interest in developing more reactive chemical systems that efficiently hydrolyze the phosphatediester bonds of DNA and RNA with sequence specificity.[19,47−50] One of the challenging problems of the elegant binuclear metal complexes is to elucidate the overall catalytic mechanism and to identify the roles of the metal ions. In general, there are three direct (inner sphere) modes of activation that a metal ion can provide for accelerating the rate of phosphate ester hydrolysis.[2] They are Lewis acid activation in which a phosphoryl oxygen coordinates to a metal, for example, the substitutionally inert binuclear Co^{III} [51−56] and Cu^{II} [7,56] complexes; nucleophile activation in which a nucleophile such as hydroxide coordinates to the metals, for example, Cu^{II} hydroxides and alkoxides;[57] and leaving group activation in which a leaving group oxygen atom coordinates to the metals.[2] DNA hydrolysis requires nucleophile activation in addition to double Lewis acid activation, while double Lewis acid activation alone is enough to rapidly hydrolyze RNA. Additionally,

(19) Schnaith, L. M. T.; Hanson, R. S.; Que, L., Jr. *Proc. Natl. Acad. Sci. U.S.A.* **1994**, *91*, 569.
(20) Westheimer, F. H. *Science* **1987**, *235*, 1173.
(21) Dervan, P. B. *Science* **1986**, *232*, 464.
(22) Burrows, C. J.; Rokita, S. E. *Acc. Chem. Res*. **1994**, *27*, 295.
(23) Mazumder, A.; Chen, C.-h. B.; Gaynor, R. B.; Sigman, D. S. *Biochem. Biophys. Res. Commun*. **1992**, *187*, 1503.
(24) Guo, Z.; Sadler, P. J. *Angew. Chem., Int. Ed. Engl*. **1999**, *38*, 1513.
(25) Oratveil, G.; Duarte, V.; Bernadou, J.; Meunier, B. *J. Am. Chem. Soc*. **1993**, *115*, 7939.
(26) Breslow, R.; Zhang, B. *J. Am. Chem. Soc.* **1994**, *116*, 7893.
(27) Takeda, N.; Irisawa, M.; Komiyama, M. *Chem. Commun*. **1994**, 2273.
(28) Schneider, H.-J.; Rammo, J.; Hettich, R. *Angew. Chem., Int. Ed. Engl.* **1993,** *32*, 1716.
(29) Takasaki, B. K.; Chin, J. *J. Am. Chem. Soc*. **1995**, *117*, 8582.
(30) Roigk, A.; Hettich, R.; Schneider, H.-J. *Inorg. Chem*. **1998**, *37*, 751.
(31) Maegley, K. A.; Admiraal, S. J.; Herschleg, D. *Proc. Natl. Acad. Sci. U.S.A.* **1996**, *93*, 8160.
(32) Matsumura, K.; Endo, M.; Komiyama, M. *Chem. Commun*. **1994**, 2109.
(33) Oh, S. J.; Song, K. H.; Park, J. W. *Chem. Commun*. **1995**, 575.
(34) De Rosch, M. A.; Trogler, W. C. *Inorg. Chem*. **1990**, *29*, 2409.
(35) Young, M. J.; Wahnon, D.; Hynes, R. C.; Chin, J. *J. Am. Chem. Soc*. **1995**, *117*, 9441.
(36) Morrow, J. R.; Trogler, W. C. *Inorg. Chem*. **1990**, *29*, 2409.
(37) Itoh, T.; Hisada, H.; Usui, Y.; Fujii, Y. *Inorg. Chim. Acta* **1998**, *283*, 51.
(38) Deal, K. A.; Burstyn, J. N. *Inorg. Chem*. **1996**, *35*, 2792.
(39) Deal, K. A.; Hengge, A. C.; Burstyn, J. N. *J. Am. Chem. Soc.* **1996**, *118*, 1713.
(40) Kovári, E.; Kramer, R. *J. Am. Chem. Soc.* **1996**, *118*, 12704.
(41) Kuo, L. Y.; Barnes, L. A. *Inorg. Chem*. **1999**, *38*, 814.
(42) Hegg, E. L.; Burstyn, J. N. *Inorg. Chem*. **1996**, *35*, 7474.
(43) Itoh, T.; Hisada, H.; Sumiya, T.; Hosono, M.; Usui, Y.; Fujii, Y. *Chem. Commun*. **1997**, 677.
(44) Sreedhara, A.; Freed, J. D.; Cowan, J. A. *J. Am. Chem. Soc.* **2000**, *122*, 8814.
(45) Wilcox, D. E. *Chem. Rev.* **1996**, *96*, 2435.
(46) Sträter, N.; Lipscomb, W. N.; Klabunde, T.; Krebs, B. *Angew. Chem., Int. Ed. Engl.* **1996**, *35*, 2024.
(47) Molenveld, P.; Kapsabelis, S.; Engbersen, J. F. J.; Reinhoudt, D. N. *J. Am. Chem. Soc*. **1997**, *119*, 2948.
(48) Yashiro, M.; Ishkuba, A.; Komiyama, M. *Chem. Commun*. **1995**, 1793.
(49) Takasaki, B. K.; Chin, J. *J. Am. Chem. Soc*. **1994,** *116*, 1211.
(50) Molenveld, P.; Engbersen, J. F. J.; Reinhoudt, D. N. *Chem. Soc. Rev.* **2000**, *29*, 75.
(51) Williams, N. H.; Chin, J. *Chem. Commun*. **1996**, 131.
(52) Williams, N. H.; Cheung, W.; Chin, J. *J. Am. Chem. Soc*. **1998**, *120*, 8079.
(53) Wahnon, D.; Lebuis, A.-M.; Chin, J. *Angew. Chem., Int. Ed. Engl.* **1995**, *34*, 2412.
(54) Connolly, J.; Kim, J. H.; Banaszczyk, M.; Drouin, M.; Chin, J. *Inorg. Chem*. **1995**, *34*, 1094.
(55) Connolly, J.; Banaszczyk, M.; Hynes, R. C.; Chin, J. *Inorg. Chem.* **1994**, *33*, 665.
(56) Young, M. J.; Chin, J. *J. Am. Chem. Soc*. **1995,** *117*, 10577.
(57) Young, M. J.; Wahnon, D.; Hynes, R. C.; Chin, J. *J. Am. Chem. Soc*. **1995**, *117*, 9441.

there are three indirect (outer sphere) modes of activation mediated by the metal ions.[2]

The efficiency of currently available chemical nucleases is impressive yet still far from that of natural enzymes. The present study reports the double-stranded DNA hydrolytic activities by a series of binuclear transition metal complexes Fe_2(DTPB)(μ-O)(μ-Ac)Cl$(BF_4)_2$, Zn_2(DTPB)Cl_4,[58] Cu_2(DTPB)Cl_4, Fe_2(IDB)$_2$(μ-O)(μ-Ac)$_2Cl_2$ (IDB = *N*,*N*-bis(2′-benzimidazol-2-ylmethyl) amine),[59] Fe_2(EGTB)(Im^-)Cl_5 and Fe_2(EGTB)Cl_6, Cu_2(EGTB)(Im^-)Cl_3 and Cu_2(EGTB)-$(NO_3)_4$ (EGTB = *N*,*N*,*N*′,*N*′-tetra(2′-benzimidazol-2-yl-methyl)-1,4-bis(ethylamino)-bis(ether), Im^-= benzimidazole anion), Zn[Zn_2(TTHA)] (TTHA = triethylene tetraamine-hexaacetic acid), and Zn_2(EDTB)Cl_4 (EDTB = *N*,*N*′-bis(2′-benzimidazol-2-ylmethyl)-ethylenediamine). These binuclear complexes have significant differences in composition and structural features such as geometry, μ-oxo bridge, kinetically labile ligands, and coordination unsaturation. We expect to understand the most important composition and structural factors that can dominate the DNA hydrolytic efficiency through this study. The present data show that the diiron complex Fe_2(DTPB)(μ-O)(μ-Ac)Cl$(BF_4)_2$, designed as a model for the diiron active site in mammalian purple acid phosphatase (PAP), is the most efficient promoter for DNA hydrolytic cleavage under physiological conditions. Now, we will first describe the spectroscopic studies about the binuclear structure of, and the DNA binding and cleavage by, Fe_2(DTPB)(μ-O)(μ-Ac)Cl$(BF_4)_2$. Then, the DNA hydrolytic activity of the diiron complex will be compared with other binuclear transition metal complexes. The composition and structural factors affecting the DNA hydrolytic activity and their implications in rational designs of binuclear transition metal complexes that efficiently hydrolyze double-stranded DNA will also be discussed.

Experimental Section

Materials and Equipment. The synthesis, structures, and some properties for some of the binuclear transition metal complexes used to explore the DNA hydrolytic activities are reported elsewhere.[58,59] Calf thymus DNA was purchased from Sigma and purified using the standard procedures.[60] The DNA concentration (in base pair) was determined according to the DNA absorption at 260 nm.[61] Plasmid pBR322 DNA was purchased from Sino-American Biotechnology. [γ-^{32}P]-ATP was obtained from Gibco brl. 5′-End DNA labeling system, DNase I, T4 DNA ligase, T4 polynucleotide kinase, and restriction enzymes EcoR I, Pvu II, Hind III, Hind III DNA markers, as well as pGEM DNA markers, were purchased from Promega. All other reagents utilized were from commercial sources. The UV−vis absorption spectra were measured on a Perkin-Elmer Lambda Bio 4.0 spectrophotometer. The fluorescence and polarized fluorescence determinations were performed on a Shimadzu RF-540 spectrophotometer. The infrared spectra (IR) were recorded in the range 4000−200 cm^{-1} with a Bruker Equinox 55 Fourier transformation infrared spectrophotometer. All nuclear magnetic resonance (NMR) experiments were performed on a Bruker AMX 500 MHz NMR spectrometer. The electron spin resonance (ESR) spectra at X-band were obtained with a Bruker 200D-SRC ESR spectrometer using a methanol solution at 110 K. Cyclic voltammetry was performed with a BSA-100 electrochemical analyzer at ambient temperature in methanol using a three-electrode system; that is, a glassy carbon electrode serves as the working electrode, a platinum wire as the counter electrode, and a saturated calomel electrode as the reference. The HPLC experiments were carried out on a Waters 586 HPLC system in combination with a reversed-phase Jupiter 5 μm C18 300A column. The peak detection was performed online with a Waters 486 detection system.

Preparation of the Ligand DTPB and the Complex Fe_2(DTPB)-(μ-O)(μ-Ac)Cl$(BF_4)_2\cdot 3CH_3OH$. According to a similar program reported previously,[58] the unsymmetric binuclear ligand DTPB was prepared by a modified method. The mixture of diethyl enetriamine-*N*,*N*,*N*′,*N*″,*N*″-pentaacetic acid and *ortho*-phenylene diamine in a 1:5 molar ratio was heated to 140−200 °C in glycol(1,2-diethanol) and refluxed for 4−8 h. After cooling to room temperature, a violet-red product was produced. The product was dissolved in ethanol, decolorized with charcoal, and precipitated with cooling diethyl ether. A pale yellow precipitate was filtered and washed thoroughly with diethyl ether. A white powder was obtained by twice recrystallizing the yellow crude product from absolute ethanol and dried in a vacuum with a final yield 80%. ^{1}H NMR spectroscopy of the ligand $C_{44}H_{43}N_{13}\cdot 3H_2O$ is identical with that previously described,[58] that is, δ (ppm, d_6-dimethyl sulfoxide, TMS): 13.10 (broad, 5H), 7.60 (medium, 10H), 7.20 (medium, 10H), 4.05 (strong, 10H), 2.80 (strong, 8H).

The DTPB (2.00 g, 2.50 mmol) and $FeCl_3\cdot 6H_2O$ (1.44 g, 5.34 mmol) was dissolved in refluxing methanol (50 mL), respectively, followed by mixing to give a dark red solution. Excess of sodium acetate $NaAc\cdot 3H_2O$ (0.40 g, 4.88 mmol) and $NaBF_4$ (0.90 g, 8.18 mmol) was added into the solution and stirred overnight at room temperature. The mixture solution was concentrated by natural evaporation, and a slurry of a dark red product was obtained. The product was dissolved in methanol and dried with anhydrous Na_2SO_4. After filtering, the filtrate was collected and concentrated under reduced pressure to afford a purple-red solid. The powder product was recrystallized with methanol and dried under vacuum. Calcd elemental analysis (%) of the product for $Fe_2C_{49}H_{58}N_{13}O_6B_2F_8Cl$: C, 47.24; H, 4.69; N, 14.61. Found: C, 47.21; H, 4.89; N, 14.16. Molar conductivity Λ_m: 222 S cm^2 mol^{-1} (1:3 type). UV−vis spectrum in methane λ_{max}/nm (ϵ_m/l cm^{-1} mol^{-1}): 227 (37 600) and 283 (33 700) attributed to the $\pi \rightarrow \pi^*$ transition of the ligand; 302 (13 900) and 490 (shoulder, 821) attributed to the ligand to metal charge transfer. IR (Nujol, cm^{-1}): 3419−3060 (broad and strong), O−H of methanol and N−H and C−H of aromatic ring; 2918 (medium), =CH_2; 1624 (medium) and 749 (strong), skeletal and folding of aromatic ring, respectively; 1391 (medium) and 1273 (medium), amino and aliphatic C=N, respectively; 1521 (medium) and 1458 (strong), the asymmetric and symmetric μ-bridged acetate ion, respectively; 820 (weak) and 524 (weak), the asymmetric and symmetric Fe−O−Fe; 431, Fe−O; 290, Fe−N; 1083, BF_4^{-1}. ^{1}H NMR: δ (ppm, D_2O), 12.10 (broad, 5H); 7.7−7.2 (medium, 20H); 4.9 (broad, H_2O); 3.60, 3.36, and 1.17 (CH_3OH); 8.35 (weak) and 2.15 (CH_3COO^{1-}). ESR: *g*, 8.88, 5.36, 4.27, 2.02. Cyclic voltammetry: E_c, 210 mV, i_c, 3.8 μA; E_a, 500 mV, i_a, 2.9 μA.

UV−Visible Absorption Spectra. The spectra of Fe_2(DTPB)-(μ-O)(μ-Ac)Cl$(BF_4)_2$ in the absence of DNA were recorded in 0.1

(58) Birker, P. J. M. W. L.; Schierbeek, A. J.; Verschoor, G. C.; Reedijk, J. *J. Chem. Soc., Chem. Commun*. **1981**, 1124.
(59) Liao, Z.; Xiang, D.; Li, D.; Chen, X.; Mei, X. *Synth. React. Inorg. Met.-Org. Chem*. **2000**, *30*, 683.
(60) Sambrook, J.; Fritsch, E. F.; Maniatis, T. *Molecular cloning: a laboratory manual*, 2nd ed.; Cold Spring Harbor Laboratory Press: Plainview, NY, 1989.
(61) Ausubel, F. M.; Brent, R.; Kingston, R. E.; Moore, D. D.; Seidman, J. G.; Smith, J. A.; Struhl, K. *Short protocols in molecular biology*, 3rd ed.; John Wiley & Sons: New York, 1995.

M NaH_2PO_4/Na_2HPO_4 or NaAc/HAc buffers by varying pH, utilizing the buffers as controls. The spectra of the diiron complex in the presence of DNA were measured after incubating their mixtures in 0.01 M pH 7.0 Tris·Cl buffer for 1 h at 37 °C, where the controls were the corresponding DNA solutions. The DNA absorption spectra with increasing concentration of the diiron complex were determined after incubating their mixtures in 0.01 M pH 7.0 Tris·Cl buffer for 1 h at 37 °C, where the controls are the corresponding Fe_2(DTPB)(μ-O)(μ-Ac)Cl$(BF_4)_2$ solutions. To obtain practical DNA-mediated hypochromic spectra of the diiron complex absorbance, the following measurements were performed: (1) the absorption spectra of DNA mixtures with the diiron complex utilizing the diiron complex solution as the control (Figure 3), (2) the absorption spectra of the diiron complex in the absence of DNA, (3) the absorption spectra of the diiron complex in the presence of DNA, (4) practical DNA-mediated hypochromic spectra of the diiron complex by subtracting spectra (3) from spectra (2). The spectral characterization is based on the following mathematical relationship and can cancel the influence of the spectroscopic superposition between DNA and the diiron complex on the hypochromism of the diiron complex absorbance. If $A_{DNA(com)}$ and A_{com} are regarded as the DNA absorbance in the pesence of the diiron complex and the diiron complex alone, we have the equation (corresponding to Figure 3)

$$A_{DNA(com)} = A_{DNA+com} - A_{com} \quad (1)$$

Here, $A_{DNA+com}$ is the absorbance for the DNA mixture with the diiron complex. $A_{DNA+com}$ is equal to the sum of the practical DNA absorbance ($A^o_{DNA(com)}$) in the presence of the diiron complex and the practical absorbance ($A^o_{com(DNA)}$) of the diiron complex in the presence of DNA, that is,

$$A_{DNA(com)} = A^o_{DNA(com)} + A^o_{com(DNA)} - A_{com} \quad (2)$$

Here, $A^o_{DNA(com)}$ and $A^o_{com(DNA)}$ reflect the DNA interaction with the diiron complex and cannot be determined. Equation 2 is rearranged:

$$A_{DNA(com)} - A^o_{DNA(com)} = A^o_{com(DNA)} - A_{com} = -(A_{com} - A^o_{com(DNA)}) \quad (3)$$

The hypochromism is a difference between the absorbance of Fe_2(DTPB)(μ-O)(μ-Ac)Cl$(BF_4)_2$ alone and that of the DNA−Fe_2(DTPB)(μ-O)(μ-Ac)Cl$(BF_4)_2$ mixture utilizing the corresponding DNA solution as controls. Equation 4 represents the absorbance hypochromism (A_{hypo}) for the diiron complex mediated by DNA, where $A_{com(DNA)}$ is the absorbance of the diiron complex in the presence of DNA.

$$\begin{aligned} A_{hypo} &= A_{com} - A_{com(DNA)} = A_{com} - (A_{com+DNA} - A_{DNA}) \\ &= A_{com} - [(A^o_{com(DNA)} + A^o_{DNA(com)}) - A_{DNA}] \\ &= (A_{com} - A^o_{com(DNA)}) + (A_{DNA} - A^o_{DNA(com)}) \end{aligned} \quad (4)$$

Equation 3 is replaced into equation 4:

$$\begin{aligned} A_{hypo} &= (A_{DNA} - A^o_{DNA(com)}) + (A^o_{DNA(com)} - A_{DNA(com)}) \\ &= A_{DNA} - A_{DNA(com)} = A_{com} - A_{com(DNA)} \end{aligned} \quad (5)$$

This indicates that both the DNA-mediated hypochromism of Fe_2(DTPB)(μ-O)(μ-Ac)Cl$(BF_4)_2$ absorbance and the hypochromism of DNA absorbance induced by the diiron complex are the same.

Thermal Denaturation of DNA. The absorption values of DNA as well the mixture of DNA and Fe_2(DTPB)(μ-O)(μ-Ac)Cl$(BF_4)_2$ in 0.01 M pH 7.0 Tris·Cl buffer at 260 nm were recorded by increasing 3 °C from 35 to 95 °C in a Jubalo thermostatic bath, respectively, where the controls were the buffer and the buffers in the absence and presence of the diiron complex, whose concentration was same as that in the sample.

Estimation of the Binding Constant of Fe_2(DTPB)(μ-O)(μ-Ac)Cl$(BF_4)_2$ to DNA. The polarized fluorescence was utilized to estimate the binding constant of Fe_2(DTPB)(μ-O)(μ-Ac)Cl$(BF_4)_2$ with DNA. Three sets of samples have been prepared by addition of the purified water, DNA, and 40% poly(ethylene glycol) (PEG) to the diiron complex solutions, respectively. Their luminescence intensities in the horizontal and vertical directions were recorded at 297 and 590 nm, respectively, where the exciting wavelength was 270 nm. According to the correlation equations of polarizability and anisotropy with luminescence intensities and anisotropy with the related concentrations,[62] respectively, the DNA-bound concentration of the diiron complex can be calculated. Hence, the following expression for binding constant of metal complexes to DNA can be obtained.

$$K = C_b/(C_{total} - C_b)([DNA]_o - C_b) \quad (6)$$

$[DNA]_o$ is the original DNA base pair concentration, and C_{total} and C_b are the total and DNA-bound concentrations of Fe_2(DTPB)(μ-O)(μ-Ac)Cl$(BF_4)_2$, respectively.

pBR322 DNA Cleavage Experiments by Various Binuclear Metal Complexes. The 20 μL total volume of mixtures of 77 μM pBR322 DNA with various binuclear metal complexes of 50 μM in 0.01 M pH 7.0 Tris·Cl buffer was incubated for 30 min at 37 °C. To eliminate the effect of the oxidative species which results from the oxygen dissolved in the solutions on the hydrolysis reactions, the incubation of all samples was performed under anaerobic conditions such as deoxygenated and highly purified water, isolation from air, and in argon or nitrogen atmosphere. The hydrolysis reactions were quenched by addition of 4 μL 5× TBE (89 mM Tris, 89 mM boron hydroxide, 2 mM EDTA) sample buffer containing xylene cyanol and bromophenol blue. The electrophoresis of DNA cleavage products was performed on 1% agarose gel. The gels were run at 75 V for 45 min in 0.01 M pH 7.0 NaH_2PO_4/Na_2HPO_4 buffer. To perform a simple kinetic analysis, the electrophoresis bands were visualized by staining in an ethidium bromide solution and photographed with Kodak films on a UV transilluminator at 254 nm. The photographic negatives were scanned on a UVR scanner set on transmission mode. The public program LandLeader version 3.0 was used to evaluate the relative amounts of the supercoiled and linear forms of DNA.

HPLC Detection of CT DNA Cleavage Products with Fe_2(DTPB)(μ-O)(μ-Ac)Cl$(BF_4)_2$. In each parallel experiment, 5 μL of the reaction mixture (0.12 mM calf thymus DNA and 0.08 mM Fe_2(DTPB)(μ-O)(μ-Ac)Cl$(BF_4)_2$ in 0.01 M pH 7.0 Tris·Cl buffer after incubating 12 h at 37 °C, respectively) was injected into the column at 35 °C and eluted by a flow phase consisting of 5% methanol and 95% pH 4, 0.05 M KH_2PO_4 at a flow rate of 1.0 mL/min.

Ligation Experiment on the pBR322 DNA Linearized by Fe_2(DTPB)(μ-O)(μ-Ac)Cl$(BF_4)_2$. First, the linear DNA was isolated from the pBR322 DNA cleavage products provided by Fe_2(DTPB)(μ-O)(μ-Ac)Cl$(BF_4)_2$. Then, in each parallel experiment, the 20 μL total volume of mixtures containing 2 μL 10× ligation

(62) Lakowicz, J. R. *Principles of fluorescence spectroscopy*; Plenum: London, 1983.

buffer, 1 μL 0.1 M ATP, 4 μL 40% PEG, and 3 Weiss units T4 DNA ligase reacted with the linear DNA for 24 h at room temperature. The ligation products were monitored by the electrophoresis and visualized by staining in an ethidium bromide solution.

5′-End-Labeling of Fe_2(DTPB)(μ-O)(μ-Ac)$Cl(BF_4)_2$-Broken DNA Fragments. First, 77 μM supercoiled pBR322 DNA in 50 μL 0.01 M pH 7.0 Tris·Cl buffer was hydrolytically cleaved by 50 μM Fe_2(DTPB)(μ-O)(μ-Ac)$Cl(BF_4)_2$ for 1 h at 37 °C. Then, the linearized pBR322 DNA isolated from the reaction mixture was concentrated and followed by treatment with calf intestinal alkaline phosphatase. Third, the linear plasmid was 5′-end-labeled with T4 polynucleotide kinase and [γ-^{32}P]-ATP. After labeling, the DNA was finally digested with EcoR I and Pvu II restriction endonucleases. The digested products were separated by 12% (w/v) denaturing polyacrylamide gel electrophoresis and visualized by an autoradiography.[60,61] Here, pGEM DNA markers and Hind III markers were utilized as the controls.

Cleavage of pBR322 DNA Restriction Fragments and Determination of Cleavage Sites. A 3710 bp pBR322 DNA restriction fragment (sequence 650−4360) was isolated according to the standard isolation procedures.[60,61] The 77 μM DNA was 5′-^{32}P end-labeled with T4 polynucleotide kinase and [γ-^{32}P]-ATP. One of the DNA fragments was incubated with Fe_2(DTPB)(μ-O)(μ-Ac)-$Cl(BF_4)_2$ (80 μM) in 50 μL of 0.01 M pH 7.0 Tris·Cl buffer at 37 °C for 2 h. Another DNA sample was treated with 40 units of DNase I for 3 min at room temperature. Digestion was quenched by addition of the 10 μL solution containing 50 mM EDTA, 0.5% (w/v) sodium dodecyl sulfate (SDS), 1.8 M sodium acetate, and 10 μg yeast tRNA. The cleaved DNA was ethanol precipitated, dried, and dissolved in 3 of 95% (v/v) formamide/H_2O containing 0.05% (w/v) xylene cyanol and 20 mM EDTA. They were heated at 95 °C for 10 min and loaded onto 12% (w/v) denaturing polyacrylamide gel. After the gel was dried, autoradiography was carried out at −80 °C without using intensifying screen.

Footprinting Analysis of Fe_2(DTPB)(μ-O)(μ-Ac)$Cl(BF_4)_2$ Bound DNA Sequence. The 5′-^{32}P labeled 3710 bp pBR322 DNA restriction fragment (77 μM) was incubated with Fe_2(DTPB)(μ-O)(μ-Ac)$Cl(BF_4)_2$ with varied concentrations (10−80 μM) in 50 μL of 0.01 M pH 7.0 Tris·Cl buffer at 37 °C for 3 min. Such a short reaction time allows that the diiron complex sufficiently binds to DNA and the DNA is not degraded significantly. Then, 40 unit of DNase I was added and treated for 3 min at room temperature.[60,61] The following procedures were as described previously.

Results

Binuclear Structure of Fe_2(DTPB)(μ-O)(μ-Ac)$Cl(BF_4)_2$. The binuclear structure of Fe_2(DTPB)(μ-O)(μ-Ac)$Cl(BF_4)_2$ was characterized by various spectral methods. Unfortunately, we were unsuccessful in our attempt to obtain its X-ray crystal diffraction structure owing to its unsymmetric property. In the IR spectrum, the peaks at 1521 and 1458 cm^{-1} are attributed to the asymmetric and symmetric stretching vibration of the μ-bridged acetate, and the bands at 820 and 524 cm^{-1} are the asymmetric and symmetric stretching vibration of the group Fe−O−Fe. The ^{1}H NMR at 8.35 and 2.15 ppm can be also ascribed to the μ-bridged acetate. In the ESR spectrum, the sharp signal observed at $g = 4.27$ ($S = {}^5/_2$) and the signal at $g = 2.02$ ($S = {}^1/_2$) are characteristic of a high-spin non-heme ferric system with rhombic symmetry, and the signal at $g = 5.36$ is due to Fe(III) with axial symmetry. High-spin octahedral Fe(III) complexes normally exhibit g values close to free spin in their ESR spectra, but highly distorted six-coordinate environments are known to result in large values (such as $g = 8.88$).[63,64] All these data provide an essential support to the binuclear structure of Fe_2(DTPB)(μ-O)(μ-Ac)$Cl(BF_4)_2$. Indeed, the ligand DTPB is one that can coordinate to two metal atoms.

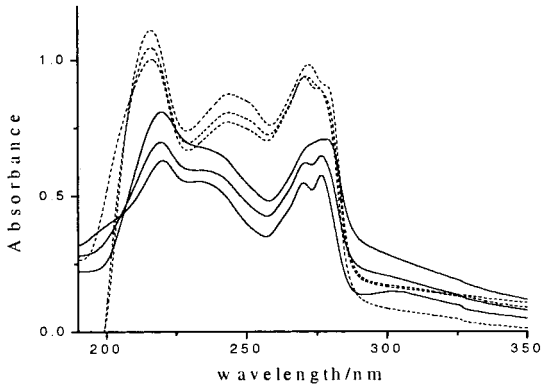

Figure 1. Absorption spectra of 40 μM Fe_2(DTPB)(μ-O)(μ-Ac)$Cl(BF_4)_2$ in 0.1 M NaH_2PO_4/Na_4HPO_4 buffer (dotted lines, pH 6, 7, 8) and in 0.1 M HAc/NaAc buffer (solid lines, pH 4, 5, 6). The controls are the corresponding pH buffers.

DNA Binding by Fe_2(DTPB)(μ-O)(μ-Ac)$Cl(BF_4)_2$. Several different assays were employed to determine the extent of Fe_2(DTPB)(μ-O)(μ-Ac)$Cl(BF_4)_2$ binding to DNA. An important change in the absorption spectra of Fe_2(DTPB)-(μ-O)(μ-Ac)$Cl(BF_4)_2$ in the buffers (Figure 1) is that all bands blue-shifted compared to that in methane. On the other hand, a common alteration in the absorption spectra of the diiron complex in the different buffers is that its absorbance progressively decreases and the bands at ∼218 and ∼278 nm, attributed to the ligand to metal charge transfer, become distinct by decreasing pH. The prominent spectral differences in these two buffers are (1) that the isosbestic points of the diiron complex in the absence of DNA are evident at 206 nm in the NaH_2PO_4/Na_2HPO_4 buffer and at 210 nm in the HAc/NaAc buffer, (2) that the absorbance in the former buffer is stronger than that in the latter buffer, and (3) that the absorption platform at ∼238 nm in the HAc/NaAc buffer, ascribed to the $\pi \rightarrow \pi^*$ transition of the ligand, is inverted into a large and observable peak at ∼242 nm in the NaH_2PO_4/Na_2HPO_4 buffer. These indicate that two kinds of the diiron complexes are in equilibrium. Moreover, the two kinds of complexes involved in the equilibrium in HAc/NaAc buffer may be different from that in NaH_2PO_4/Na_2HPO_4 buffer. The phosphate or acetate in the buffers may enter into the first ligand sphere of the ferric ion. The absorption spectra are strongly affected by binding to DNA, resulting in substantial hypochromism and shifts to longer wavelength of the strongest $\pi \rightarrow \pi^*$ transition of the ligand, although the overall absorbance profile is similar to that in NaH_2PO_4/Na_2HPO_4 buffer, as shown in Figure 2 and Table 1. Moreover, the hypochromism is in good proportion to the DNA concentra-

(63) Constable, E. C.; Ward, M. D.; Tocher, D. A. *J. Chem. Soc., Dalton Trans.* **1991**, 1675.
(64) Neto, L. M.; Tabak, M.; Nascimento, O. R. *J. Inorg. Biochem.* **1990**, *40*, 309.

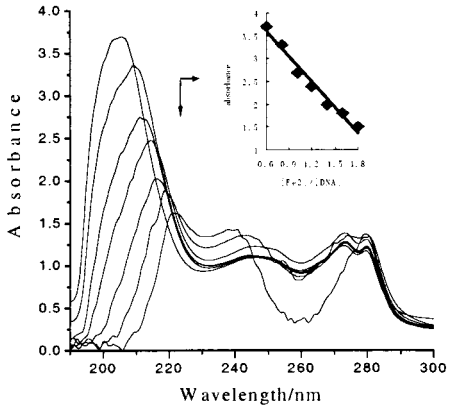

Figure 2. Absorption spectra of 40 μM Fe_2(DTPB)(μ-O)(μ-Ac)Cl(BF_4)$_2$ by increasing the molar concentration ratio of DNA to the diiron complex of 0.6−1.8 in 0.01 M pH 7.0 Tris·Cl buffer, where the controls were the corresponding DNA solutions.

Table 1. DNA-mediated Hypochromism of Absorbance of [Fe_2(DTPB)(μ-O)(μ-Ac)Cl](BF_4)$_2$

	[DNA]/[[Fe_2(DTPB)-(μ-O)(μ-Ac)Cl](BF_4)$_2$]	hypochromism (%)	shift in strongest benizimidazolyl-centered transition
apparent	0.6−1.8	60	207 → 222 nm, red shift
practical	0.6−1.8	83	209 → 204 nm, blue shift

tions (Figure 2). Nevertheless, we propose that this is an apparent phenomenon and does not reflect the true DNA-mediated hypochromism of the diiron complex because of the superposition between their absorbances. On the other hand, the estimation of the binding constant, $K = (1.1 \pm 0.2) \times 10^5$ M, by the polarized fluorescence indicates the binding interaction between DNA and the diiron complex.

The influence of Fe_2(DTPB)(μ-O)(μ-Ac)Cl(BF_4)$_2$ on the DNA absorbance was examined. Initially, it has been found that the diiron complex results in a significant hypochromism (46%) in the strongest DNA absorption band (Figure 3). When the concentration ratio of the diiron complex to DNA is 1.8−2.1, the mixture system exhibits its minimum absorbance. These facts suggest (1) the reaction of DNA with the diiron complex reaches equilibrium at the concentration ratio, and (2) the DNA is saturated by the diiron complex when the ratio is more than 1.8. However, the DNA absorption spectra become remarkably sophisticated and lose regularity by increasing the concentration ratio (data not shown). Obviously, this puzzled alteration is produced by the difference of the diiron complex absorbances between in the sample and in the control, and it demonstrates a phenomenon that the endless increase in concentration of a metal complex cannot induce a limitless decrease in the DNA absorbance.

The DNA-mediated hypochromic spectra of the diiron complex were obtained according to the previously described method for spectral characterization, as shown in Table 1. The hypochromic spectra are in essence different from Figures 2 and 3. Obviously, the hypochromism is larger than that shown in Figures 2 and 3, because the figures are a result of superposition of both the DNA-mediated hypochromism in Fe_2(DTPB)(μ-O)(μ-Ac)Cl(BF_4)$_2$ and the DNA absorbance, or vice versa. In addition, a large red shift in the strongest $\pi \rightarrow \pi^*$ transition of the ligand in Figure 3 is inverted into a slight blue shift. These results reveal that general absorption spectroscopy cannot differentiate the influences on each other between DNA and a metal complex when their spectroscopic superposition heavily occurs.

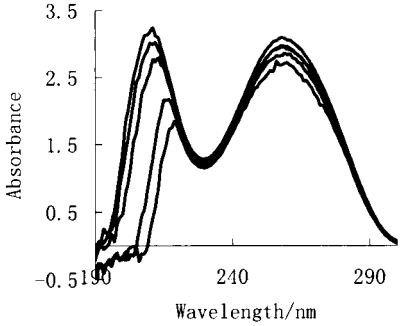

Figure 3. Absorption spectra of 3 μM DNA by increasing the molar concentration ratio of Fe_2(DTPB)(μ-O)(μ-Ac)Cl(BF_4)$_2$ to DNA of 0.6−1.8 in 0.01 M pH 7.0 Tris·Cl buffer, where the controls are the corresponding Fe_2(DTPB)(μ-O)(μ-Ac)Cl(BF_4)$_2$ solutions.

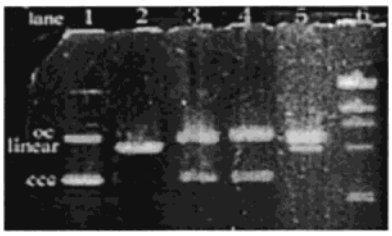

Figure 4. Agarose gel electrophoresis of pBR322 DNA cleavage in 0.01 M pH 7.0 Tris·Cl buffer (ethidium bromide staining). Reaction conditions: 77 μM DNA base pairs, 37 °C for 3 h; lane 1, control; lane 2, by EcoR I; lane 3, by 0.1 M Fe^{2+}; lane 4, by 0.1 M Fe^{3+}; lane 5, by 50 μM Fe_2(DTPB)-(μ-O)(μ-Ac)Cl(BF_4)$_2$ and 0.05 M EDTA; lane 6, by 50 μM Fe_2(DTPB)-(μ-O)(μ-Ac)Cl(BF_4)$_2$; lane 7, λ/HinD III DNA marker.

The Fe_2(DTPB)(μ-O)(μ-Ac)Cl(BF_4)$_2$ binding can generally affect the DNA double helix stability, that is, DNA denaturation temperature. Hence, the influence of the diiron complex on DNA denaturation temperature was observed. The result indicates that the temperature rises from 73−76 °C to 79−83 °C. Moreover, it was not found that the curve was obviously changed. These data imply that Fe_2(DTPB)-(μ-O)(μ-Ac)Cl(BF_4)$_2$ neither unwinds the DNA double helix nor produces DNA oxidative cleavage products such as free base. Therefore, the combination of the DNA denaturation temperature data with the previously described spectral data provides a suggestion that the diiron complex may directly bind to the DNA phosphate backbone, because the interaction neutralizes the negative charges on DNA backbone.

pBR322 DNA Cleavage Experiments by Fe_2(DTPB)-(μ-O)(μ-Ac)Cl(BF_4)$_2$. The DNA cleavage behavior with Fe_2(DTPB)(μ-O)(μ-Ac)Cl(BF_4)$_2$ under physiological conditions (pH 7, 37 °C) has been observed by the transformation of the supercoiled form (CCC) to the nicked (OC) and linear forms of plasmid DNA. Figure 4 shows the cleavage reactions of pBR322 DNA mediated by a variety of scission systems containing iron. It is clear from lanes 4−6 that the diiron complex alone exhibits a significant cleavage in the highest known concentration ratio of DNA to the diiron complex (77:50), while Fe^{3+} ion alone as well as the mixture of Fe_2(DTPB)(μ-O)(μ-Ac)Cl(BF_4)$_2$ with EDTA do not

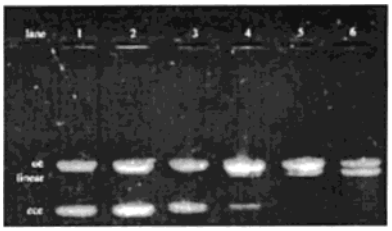

Figure 5. Time-dependence of pBR322 DNA (77 μM DNA base pairs) cleavage by 100 μM Fe_2(DTPB)(μ-O)(μ-Ac)Cl(BF_4)$_2$ in 0.01 M pH 7.0 Tris·Cl buffer at 37 °C: lane 1, control; lane 2, 3, 4, 5, 6, reaction for 5, 10, 20, 30, 60 min, respectively.

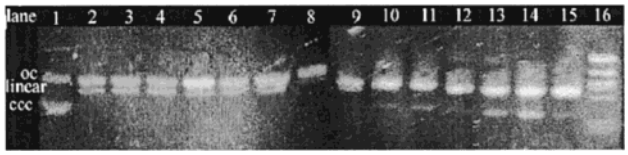

Figure 6. Ion strength dependence of pBR322 DNA (77 μM DNA base pairs) cleavage by 50 μM Fe_2(DTPB)(μ-O)(μ-Ac)Cl(BF_4)$_2$ in 0.01 M pH 7.0 Tris·Cl buffer at 37 °C for 30 min: lane 1, DNA control; lanes 2−15, with 0, 5, 25, 50, 100, 150, 200, 300, 400, 500, 600, 700, 800 mM NaCl added to cleavage buffer, respectively; lane 16, λ/HinD III DNA markers.

display an observable cleavage. These results indicate that the DNA cleavage activity by the diiron complex can be ascribed to the cooperative effect between the two Fe^{3+} ions and their ligands.

The cleavage experiments of pBR322 DNA of Fe_2(DTPB)-(μ-O)(μ-Ac)Cl(BF_4)$_2$ under different conditions have been carried out. Increasing temperature or increasing concentration results in more efficient cleavage. The concentration of the diiron complex that can efficiently promote the DNA cleavage can be lowered to 10 μM under mild conditions. The time dependence of DNA cleavage reveals that the supercoiled form completely disappears after 30 min, as shown in Figure 5. The observed distribution of supercoiled and linear DNA in the agarose gels provides a measure of the extent of hydrolysis of the phosphodiester bonds in each plasmid DNA, and we used these data to perform simple kinetic analysis. Measurement of both the rate of appearance of linear DNA and the rate of disappearance of supercoiled DNA indicated that the approximate pseudo-first-order rate constants are 2.1×10^{-3} s^{-1} and 1.2×10^{-3} s^{-1}. This is one of the largest known rate enhancement factors of $\sim 10^{10}$ against DNA. This rate acceleration may be due to the combination of Lewis acid activation ($<10^2$) and intramolecular nucleophile activation ($\sim 10^8$).

On the other hand, the ionic strength does not exert observable influence on the cleavage reaction (Figure 6). This implies that the electrostatic interaction between the diiron complex and the DNA is not a principal factor responsible for the degradation reaction. However, the DNA cleavage reactions at various pH values and in different media demonstrate that the DNA cleavage efficiency obviously increases with decreasing pH (Figure 7). In addition, at pH 4.0, the clear agarose electrophoretic bands completely disappear, and a smear occurs. The DNA cleavage in Tris·Cl medium is more observable than in the phosphate buffer at pH 7.0, while the DNA cleavage in the phosphate and acetate buffers exhibits a negligible difference at pH 6.0.

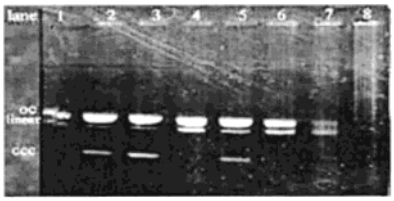

Figure 7. Cleavage of pBR322 DNA by 50 μM Fe_2(DTPB)(μ-O)(μ-Ac)-Cl(BF_4)$_2$ at various pH values and in different media. Reaction conditions: 77 μM DNA base pairs, 37 °C for 3 h; lanes 1, 2, 3, in 0.01 M pH 7.0, 8.0, 9.0 Tris·Cl buffer, respectively; lanes 4, 5, in 0.01 M pH 6.0, 7.0 NaH_2PO_4/Na_2HPO_4 buffer, respectively; lanes 6, 7, 8, in 0.01 M pH 6.0, 5.0, 4.0 HAc/NaAc buffer, respectively.

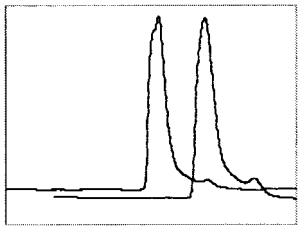

Figure 8. HPLC chromatograms showing calf thymus DNA cleavage by Fe_2(DTPB)(μ-O)(μ-Ac)Cl(BF_4)$_2$ (upper curve); lower curve is the control.

These phenomena suggest that the phosphate or acetate may competitively bind to the two metal ions in Fe_2(DTPB)(μ-O)(μ-Ac)Cl(BF_4)$_2$ with DNA phosphate.

To explore the DNA cleavage mechanism by Fe_2(DTPB)-(μ-O)(μ-Ac)Cl(BF_4)$_2$, the DNA cleavage chemistry in the presence of oxygen free radical scavengers and under anaerobic conditions has been examined (data not shown). The free radical scavengers such as dimethyl sulfoxide, poly(ethylene glycol), and mannitol do not present any observable inhibition on the DNA cleavage reactions, whereas poly(ethylene glycol) can even enhance the reactivity of the diiron complex. Moreover, the absence of oxygen can exert only negligible influence on the DNA cleavage chemistry. In contrast, the DNA oxidative degradation mediated by $Fe(EDTA)^{2-}/H_2O_2$ is almost completely inhibited by the free radical scavengers or under anaerobic conditions. Thus, it is presumable that the DNA cleavage by Fe_2(DTPB)(μ-O)(μ-Ac)Cl(BF_4)$_2$ is not involved in oxygen free radical pathway.

The DNA non-oxidative cleavage by Fe_2(DTPB)(μ-O)(μ-Ac)Cl(BF_4)$_2$ is supported by the HPLC experiments (Figure 8). Any significant and new peak has not been observed in the reversed-phase HPLC for the mixture of calf thymus DNA and Fe_2(DTPB)(μ-O)(μ-Ac)Cl(BF_4)$_2$ after 12 h at pH 7.0 and at 37 °C, although the agarose electrophoretic results show the DNA complete cleavage (data not shown). Obviously, this is due to the DNA hydrolytic cleavage products with the same 3′-OH and 5′-OPO_3 ends and greatly decreasing sizes, thereby their hydrophobicity is slightly changed (retention time from 3.15 and 4.15 min for the control to 3.13 and 4.13 min for the sample). However, the slight alteration of hydrophobicity results in an observable shoulder accompanying with the main peak at 3.13 min relative to the original DNA peak (Figure 8). Taken together, all the above-mentioned data suggests that both supercoiled and usual double-stranded DNA cleavage mediated by the diiron complex can occur by a non-oxidative mechanism.

Table 2. PBR322 DNA Cleavage by Various Binuclear Metal Complexes (% Estimated)

	DNA forms		
	supercoiled	nicked	linear
$[Fe_2(DTPB)(\mu\text{-}O)(\mu\text{-}Ac)Cl](BF_4)_2$	8	51	41
$Zn_2(DTPB)Cl_4$	30	42	28
$Zn_2(EDTB)Cl_4$	41	45	14
$Fe_2(EGTB)Cl_6$	38	48	14
$[Fe_2(IDB)_2(\mu\text{-}O)(\mu\text{-}Ac)_2]Cl_2$	23	70	7
$Cu_2(DTPB)Cl_4$	37	44	21
$Cu_2(EGTB)(NO_3)_4$	49	51	
$Zn[Zn_2(TTHA)]^a$	49	51	
$Cu_2(EGTB)(Im^-)Cl_3$	57	43	
$Fe_2(EGTB)(Im^-)Cl_5$	58	42	
control	62	38	

[a] From another agarose gel electophoresis experiment.

Comparison of DNA Cleavage chemistry by Various Binuclear Metal Complexes. Table 2 displays the reaction results after the incubation of various binuclear metal complexes with plasmid DNA for 30 min under physiological conditions (pH 7.0, 37 °C). All the DNA cleavage processes might occur via a non-oxidative pathway, because (1) no co-cleavage agent is added to these systems, (2) the reactions proceed under the anaerobic conditions, and (3) these binuclear metal complexes contain not only oxidative metal ions, but also non-oxidative ones, and it has not been observed that all the former complexes show more effective DNA cleavage chemistry than all the latter.

Table 2 shows that the DNA cleavage efficiency exhibited by various binuclear metal complexes is very different. It is clear from lane 10 that $Fe_2(DTPB)(\mu\text{-}O)(\mu\text{-}Ac)Cl(BF_4)_2$ results in the nearly complete disappearance of the supercoiled form and the appearance of linear DNA. This illustrates that the diiron complex exhibits the most significant DNA cleavage chemistry. The occurrence of the clear linear DNA bands on lanes 6 and 7 shows that the binuclear metal complexes $M_2(DTPB)Cl_4$ (M = Cu and Zn) can effectively cleave the DNA under the identical conditions. In addition, the binuclear metal complexes $Zn_2(EDTB)Cl_4$, $Fe_2(EGTB)Cl_6$ and $Fe_2(IDB)_2(\mu\text{-}O)(\mu\text{-}Ac)_2Cl_2$ can also degrade the DNA to a certain extent. The slight smear DNA fragments that appeared in all the lanes shown that the breakage products may be ascribed to the poor selectivity of the DNA degradation. However, $Cu_2(EGTB)(NO_3)_4$, $Zn[Zn_2(TTHA)]$, $Fe_2(EGTB)(Im^-)Cl_5$, and $Cu_2(EGTB)(Im^-)Cl_3$ are not effective promoters for the DNA cleavage. As a result, the competence of the complexes for degrading DNA under the non-oxidative conditions decreases in the order of appearance of linearized DNA: $Fe_2(DTPB)(\mu\text{-}O)(\mu\text{-}Ac)Cl(BF_4)_2 > Zn_2(DTPB)Cl_4 > Cu_2(DTPB)Cl_4 > Zn_2(EDTB)Cl_4$, $Fe_2(EGTB)Cl_6 > Fe_2(IDB)_2(\mu\text{-}O)(\mu\text{-}Ac)_2Cl_2 > Zn[Zn_2(TTHA)]$, $Cu_2(EGTB)(Im^-)Cl_3$, $Fe_2(EGTB)(Im^-)Cl_5$, $Cu_2(EGTB)(NO_3)_4$. It is not difficult to understand this activity order according to the composition of ligand spheres and structures of these binuclear metal complexes (vide infra).

Ligation of the DNA Linearized by $Fe_2(DTPB)(\mu\text{-}O)(\mu\text{-}Ac)Cl(BF_4)_2$. Furthermore, the ligation experiments on the linear DNA cleavage products generated by $Fe_2(DTPB)(\mu\text{-}O)(\mu\text{-}Ac)Cl(BF_4)_2$ with T4 DNA ligase have been carried out. It was unexpectedly found that the ligation efficiency nears 100% (Figure 9). The plasmid DNA linearized by the diiron complex can be converted into the closed circular form and concatemer DNA, as observed by a shift in the electrophoresis bands. It is clear that the complete ligation of DNA fragments has to meet the condition that the DNA cleavage reaction must proceed via a hydrolytic pathway; that is, the cleavage reaction must exclusively afford the DNA products with 3′-OH and 5′-OPO_3 ends, as found for the DNA hydrolysis mediated by restriction enzymes. The fact that the ligation of the DNA fragments cleaved by $Fe_2(DTPB)(\mu\text{-}O)(\mu\text{-}Ac)Cl(BF_4)_2$ produces the concatemers less than by restriction enzymes indicates the poor sequence specificity of DNA cleavage by $Fe_2(DTPB)(\mu\text{-}O)(\mu\text{-}Ac)Cl(BF_4)_2$ and the cleavage products which do not possess the strictly matched ends and are different from the enzyme-scissile products. Consequently, it is difficult to convert the DNA cleavage products into the concatemers. These observations indicate that the DNA cleavage reaction mediated by $Fe_2(DTPB)(\mu\text{-}O)(\mu\text{-}Ac)Cl(BF_4)_2$ produces no oxidative products which cannot be ligated by T4 DNA ligase.

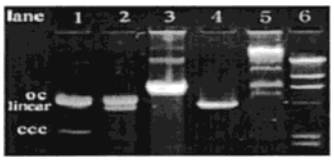

Figure 9. Ligation of pBR322 DNA cleaved by $Fe_2(DTPB)(\mu\text{-}O)(\mu\text{-}Ac)Cl(BF_4)_2$: lane 1, supercoiled (lower) and nicked (upper) pBR322 DNA; lanes 2 and 3, treatments without and with T4 DNA ligase, respectively; lane 4, linearized pBR322 DNA; lanes 5 and 6, ligation of pBR322 DNA linearized by EcoR I and EcoR V, respectively.

Table 3. ^{32}P Radioactivity Incorporation Rate (%) of PBR322 DNA Fragments Treated with $[Fe_2(DTPB)(\mu\text{-}O)(\mu\text{-}Ac)Cl](BF_4)_2$

λ/Hind III DNA markers	pGEM DNA markers	pBR322 DNA fragments linearized with $[Fe_2(DTPB)(\mu\text{-}O)(\mu\text{-}Ac)Cl](BF_4)_2$
16	23	34

Identification of DNA Cleavage Sites by $Fe_2(DTPB)(\mu\text{-}O)(\mu\text{-}Ac)Cl(BF_4)_2$. At first, an interesting phenomenon has been noticed in the course of 5′-^{32}P end-labeling of DNA fragments generated by $Fe_2(DTPB)(\mu\text{-}O)(\mu\text{-}Ac)Cl(BF_4)_2$. All the DNA fragments produced can be labeled more effectively than DNA markers, oligonucleotides, and those by the endonucleases, under the identical manipulation conditions (Table 3). It has been established that it is extremely difficult to 5′-^{32}P end-label the DNA breakage products by an oxidative pathway.[1] Hence, this fact confirms firmly that $Fe_2(DTPB)(\mu\text{-}O)(\mu\text{-}Ac)Cl(BF_4)_2$ not only breaks double-stranded DNA by a hydrolytic mechanism but also provides a large body of linearized DNA products that can be 5′-^{32}P end-labeled. Moreover, the appearance of a large body of DNA fragments capable of enzymatic manipulation is attributed to the fact that the diiron complex cleaves DNA duplex with a poor sequence specificity.

To examine further the poor sequence specificity of DNA hydrolytic breakage, we have performed the restriction analysis of the linearized pBR322 DNA by the diiron

complex. If the breakage reaction was sequence-specific, rescission of the linearized plasmid DNA with restriction endonucleases would provide the well-defined DNA fragment bands on electrophoresis. The sizes of the DNA fragments and the cleavage sites produced by Fe_2(DTPB)-(μ-O)(μ-Ac)Cl(BF_4)$_2$ can be estimated according to the location of electrophoretic bands. Thereby, the exact cleavage sites can be determined using a restriction DNA fragment as its substrate.

The result shows that a smear of the isolated linearized pBR322 DNA fragments derived from exposure to the diiron complex is observed on the gel electrophoresis experiments with the exception of a clear band at ~4.3 kbp, as expected from a random cleavage event. This fact indicates that the sizes of the products treated by Fe_2(DTPB)(μ-O)(μ-Ac)Cl-(BF_4)$_2$ are extensively distributed and the cleavage reaction occurs basically without a significant sequence specificity. The result is in agreement with the previously mentioned suggestion obtained from spectral characterization.

Determination of DNA Recognition Sequence by Fe_2(DTPB)(μ-O)(μ-Ac)Cl(BF_4)$_2$. To identify the DNA sequence recognized by the diiron complex (10−80 μM) and to confirm the inference of the DNA binding and cleavage with a poor sequence specificity, the footprinting experiments have been carried out on an 5′-^{32}P end-labeled restriction pBR322 DNA fragment (3710 bp) with DNase I (data not shown). It was found that the diiron complex cannot provide any protected region on the DNA. The result of treatment with Fe_2(DTPB)(μ-O)(μ-Ac)Cl(BF_4)$_2$ alone is similar to the pattern of the DNase I digestion. These phenomena are completely consistent with the spectral analysis that the diiron complex binds to DNA via the coordination of its two ferric ions to the oxygens on same phosphate with a poor sequence specificity. Obviously, the binding fashion could not interfere with the DNase I digestion. However, one additional finding here is that the diiron complex efficiently hydrolyzes both supercoiled DNA and linear DNA, as observed in HPLC experiments.

Discussions

DNA Binding and Cleavage by Fe_2(DTPB)(μ-O)(μ-Ac)-Cl(BF_4)$_2$. We initially expected that the benzimidazol group in the diiron complex may bind to DNA by an intercalation into DNA base pairs. However, the previously mentioned results do not support the expectation but do suggest that its two ferric ions may coordinate to two oxygens on same DNA phosphate. The coordinative interaction is facilitated because (1) the distance of ~3.1 Å between the two Fe^{3+} ions (by molecular mechanics calculation) is similar to that (3.4 Å) between two base pairs of DNA and that (3.1−3.2 Å) between the two iron atoms within mammalian PAP,[65] (2) the site coordinated by the chloride anion or the open coordination site in the diiron complex is readily substituted or occupied by the phosphate oxygens, (3) the ferric ions neutralize the negative charge on the DNA phosphate backbone. This binding interaction may occur on the DNA phosphate backbone and may not interfere with the DNA base pairing and stacking, while their exact natures remain to be determined. The coordinative interaction may lead to the consequence that the diiron complex binds to DNA with a poor sequence selectivity, because of the identity of all the phosphate groups on DNA. Thereby, it might be proposed that the diiron complex hydrolyzes DNA without sequence specificity. The proposal is in agreement with the results from both the footprinting and the restriction analysis.

Dependence of DNA Hydrolytic Cleavage Chemistry on the Compositions of Binuclear Metal Complexes. The previously described results demonstrate that the DNA hydrolytic chemistry of binuclear metal complexes is dominated by their compositions and structures. All the metal complexes that can hydrolyze DNA contain two metal ions, because there may be a concerted effect between two metal ions in the cleavage reactions.[65−67] Furthermore, the binuclear metal complexes contain a μ-oxo bridge, open coordination site(s), or/and one or more labile ligands, for example, Fe_2(DTPB)(μ-O)(μ-Ac)Cl(BF_4)$_2$ and Zn_2(DTPB)Cl_4. These facts are consistent with the previously proposed hydrolytic mechanism of phosphate diester.[65−68] The DNA hydrolytic chemistry by the binuclear metal complexes containing aromatic nitrogen heterocycles and polyamine backbone is strengthened with pH decrease. Other the other hand, the ligands with one or more negative charges cannot result in significant hydrolytic chemistry, for instance, Zn[Zn_2-(TTHA)], Cu_2(EGTB)(Im^-)Cl_3, and Fe_2(EGTB)(Im^-)Cl_5, owing to the electrostatic repulsion between DNA and the ligands.

The diiron complex Fe_2(DTPB)(μ-O)(μ-Ac)Cl(BF_4)$_2$ hydrolyzes the DNA duplex in the highest efficiency among all the binuclear metal complexes. In contrast, Fe_2(IDB)$_2$-(μ-O)(μ-Ac)$_2Cl_2$ [59] that resembles the former in composition exhibits only a weak DNA cleavage activity. The difference of ancillary ligands between them contributes to the remarkable distinction in the DNA cleavage chemistry. Although the symmetrical and stable complex Fe_2(IDB)$_2$(μ-O)(μ-Ac)$_2Cl_2$ also contains a μ-oxo bridge, it contains no labile anionic ligand and is six-coordinated and crowded in space conformation. Hence, its two ferric ions cannot coordinate directly to the DNA phosphate oxygens. This may be a critical factor that results in its poor DNA hydrolytic activity. Because there is a μ-oxo bridge in the Fe_2(EGTB)Cl_6 structure, its unstable chloride ions also cannot improve its DNA hydrolytic chemistry to the utmost extent.

There is a considerable distinction among the DNA hydrolytic chemistry exhibited by the binuclear metal complexes that contain different metal ions. The d-zinc and -copper complexes Zn_2(DTPB)Cl_4 and Cu_2(DTPB)Cl_4 can also hydrolyze DNA. However, in comparison with Fe_2(DTPB)(μ-O)(μ-Ac)Cl(BF_4)$_2$, although they are not only coordinatively unsaturated but also contain three labile Cl^-, they lack the μ-oxo bridge. This factor may produce a

(65) Lindqvist, Y.; Johansson, E.; Kaija, H.; Vihko, P.; Schneider, G. *J. Mol. Biol.* **1999**, *291*, 135.
(66) Merkx, M.; Averill, B. A. *Biochemistry* **1998**, *37*, 8490.
(67) Merkx, M.; Averill, B. A. *J. Am. Chem. Soc.* **1999**, *121*, 6683.
(68) Steitz, T. A.; Steitz, J. A. *Proc. Natl. Acad. Sci. U.S.A.* **1993**, *90*, 6498.

consequence that the zinc or cupric ions can activate the phosphate diester bonds less effectively than the ferric ions in the diiron complex. The distance between two zinc ions in $Zn_2(DTPB)Cl_4$ is ~6.9 Å,[58] whereas the corresponding distance in $Fe_2(DTPB)(\mu\text{-}O)(\mu\text{-}Ac)Cl(BF_4)_2$ is ~3.1 Å (by molecular mechanics calculation). It has been reported that if the cooperativity between two metal ions is utilized to hydrolyze phosphate diester bonds, their separation must be ~ 3.9 Å.[68] Therefore, the DNA hydrolytic activity by the binuclear zinc complex is weaker than that by the diiron complex. On the other hand, the affinity of zinc ion to DNA phosphate oxygens is larger than that of cupric ion, because copper atoms tend to coordinate to DNA bases.[69] Thus, $Zn_2(DTPB)Cl_4$ is a more efficient DNA hydrolytic agent than $Cu_2(DTPB)Cl_4$.

When studying catalytic reactions involving ligand exchange at a metal, it is important to consider the ligand exchange rates and Lewis acidity typical of that metal ion. In general, trivalent metal ions are stronger Lewis acids than divalent metal ions. However, ligand exchange reactions are generally slower at trivalent metal ions than at divalent metal ions.[70] Despite this apparent disadvantage of trivalent metal ions, several enzymes[1] are now known to make use of the strong Lewis acidity of a trivalent metal ion while exhibiting fairly high turnover numbers. The strong Lewis acidity of the ferric ions in the present study is utilized to activate the DNA hydrolysis. However, the different ligand environments allow the ferric ions to exhibit the extremely different Lewis acid activation. On the other hand, when the metal ions are bound to more anionic ligands, for example, $M_2(DTPB)Cl_4$ (M = Zn or Cu) and $Fe_2(EGTB)Cl_6$, their Lewis acidity will be decreased. This may also contribute to the low DNA hydrolytic activity. For $M_2(DTPB)Cl_4$ (M = Zn or Cu), although Lewis acidity of the former is stronger than that of the later, their DNA hydrolytic efficiency is opposite. Therefore, Lewis acidity is not a principal factor of DNA hydrolysis.

The water exchange rates for the metal ions utilized in this work decrease in the order $Cu^{2+} > Zn^{2+} \gg Fe^{3+}$.[71] At first glance, these facts seem incompatible with the results that the DNA hydrolytic activities of the binuclear metal complexes decrease in the inverse order. However, we should note that the binuclear metal complexes have different ligand environments, although some of them have the same main ligand. Moreover, the anionic ligand(s) in $Fe_2(DTPB)(\mu\text{-}O)(\mu\text{-}Ac)Cl(BF_4)_2$, $M_2(DTPB)Cl_4$ (M = Zn or Cu), and $Fe_2(EGTB)Cl_6$ can increase the rate of ligand substitution at the metal ions. The poor hydrolytic activity of $Fe_2(IDB)_2(\mu\text{-}O)(\mu\text{-}Ac)_2Cl_2$ is for lack of such an anionic ligand. As a result, we can reasonably suggest that the dominant factors for the DNA hydrolytic chemistry of the binuclear complexes are their affinities toward DNA phosphate oxygens by metal coordination, μ-oxo bridge, labile and anionic ligands, and open coordination site(s). This suggestion is supported by the three metal-substituted forms $M^{3+}Zn^{2+}$−BSPAP (M = Ga, Al, and In; BSPAP = bovine spleen PAP) for natural PAPs, because they provide enzymatic activity that is not consistent with the order of water exchange rate of $In^{3+} \gg Ga^{3+} > Al^{3+}$.[66,67]

The preceding results show that the DNA hydrolytic cleavage mechanism by $Fe_2(DTPB)(\mu\text{-}O)(\mu\text{-}Ac)Cl(BF_4)_2$ might be similar to the mechanism proposed for the mammalian[65] and plant[66,67] PAPs in its overall outline. The dinuclear metalloenzyme shows its full activity in a mixed valence Fe^{III}−Fe^{II} state (reduced state) and no activity in an oxidized state (Fe^{III}−Fe^{III}),[65] whereas the two iron atoms in the diiron complex are in the Fe^{III}−Fe^{III} state. In the DNA cleavage pathway, the function of the metal ions is to act as Lewis acids, and no free radical chemistry is involved.

Conclusions

In summary, $Fe_2(DTPB)(\mu\text{-}O)(\mu\text{-}Ac)Cl(BF_4)_2$ is effective both as a supercoiled and linear double-stranded DNA hydrolytic cleaver through Lewis acid and nucleophile activation without any requirement of co-reactants under physiological conditions. It shows the largest known rate enhancement factor of $\sim 10^{10}$ against DNA. The present study has also provided a spectral characterization method that can be utilized to directly show the binding interaction of DNA with a metal complex. The spectroscopic data suggested that the binding fashion between DNA and $Fe_2(DTPB)(\mu\text{-}O)(\mu\text{-}Ac)Cl(BF_4)_2$ might be its two ferric ions of coordination to the DNA backbone phosphate oxygens. The binding fashion leads to a consequence that the diiron complex cleaves the DNA duplex via a hydrolysis pathway with a poor sequence specificity. It has been established that dominant factors for the DNA hydrolytic activities are the μ-oxo bridge, labile and anionic ligands, and open coordination site(s) by comparisons among various binuclear metal complexes.

Acknowledgment. We thank the National Natural Science Foundation of China (Grant 29871011) and of Hubei Province of China (Grant. 987051) for their financial support.

IC010302H

(69) Sigel, H. *Chem. Soc. Rev.* **1993**, *22*, 255.
(70) Wilkins, R. G. *Kinetics and mechanism of reactions of transition metal complexes*; VCH: Weinheim, 1991; pp 199−205.
(71) Cotton, F. A.; Wilkinson, G. *Advanced inorganic chemistry*, 5th ed.; John Wiley and Sons: New York, 1988; pp 1288−1289.